Journal of The Electrochemical Society, **149** (11) A1481-A1488 (2002)
0013-4651/2002/149(11)/A1481/8/$7.00 © The Electrochemical Society, Inc.

Composition, Structure, and Electrochemical Behavior of Sol-Gel Derived Nanoparticulate Pt Thin Films

H. A. Andreas* and V. I. Birss,z**

Department of Chemistry, University of Calgary, Calgary, Alberta, Canada T2N 1N4

A Pt sol was formed using a sol-gel derived methodology. This sol, and films formed from it, were characterized using various techniques. The nanoparticulate phase, seen by transmission electron microscopy (TEM), exhibited a notable temperature dependence, with the particles averaging 1-3 nm diam when dried at room temperature and 3-6 nm diam when dried at 400°C. X-ray photoelectron spectroscopy (XPS) confirmed the presence of metallic Pt in these films. The charge density of films deposited on Au also exhibited a temperature dependence, with maximum charge densities being exhibited at *ca.* 200°C. The increase from room temperature to 200°C can be attributed to thermal conversion of residual oxidized Pt in the film to metallic Pt, as well as improved electrical connectivity between the particles due to sintering. Above 200°C, sintering becomes a major contributor to the loss of charge density, as it reduces the electroactive surface area. The efficiency of use of the metallic Pt was examined using electrochemistry and the quartz crystal microbalance technique, and was found to be 20-25%. A second phase, consisting of larger crystallites, was also found in as-formed films by both TEM and scanning electron microscopy. While this phase could be removed by rinsing with acid, it could not be identified by either X-ray diffraction or XPS.
 [DOI: 10.1149/1.1512913]

Manuscript submitted December 17, 2001; revised manuscript received May 20, 2002. Available electronically October 9, 2002.

Platinum is of great interest due to its use as an electrocatalyst for numerous reactions, examples including isobutane dehydrogenation,[1] methanol oxidation,[2,3] oxidation of methane to methanol,[4] and oxygen reduction.[5] The use of Pt as a catalyst requires that the active area remains stable with time of operation and that the expensive Pt metal is efficiently used. Thus, numerous methods to produce and utilize high surface area (usually nanoparticulate) forms of Pt have been developed, including the deposition of Pt onto porous substrates, such as zeolites or gas diffusion backings,[1,6] reduction of Pt salts using various reducing agents to produce a nanoparticulate powder,[7-11] mixing Pt black with carbon powder and/or Nafion[3,12-16] and its incorporation into polymeric matrices.[17]

In our previous work with Ir, it was found that using the same approaches as employed in sol-gel (SG) synthesis of metal oxides allowed for the preparation of highly porous, nanoparticulate (down to 1 nm diam) metallic Ir films[18] through an electrochemical reduction process. Thus, our goal has been to achieve the same outcome with Pt. In this work a derivative of the alkoxide route is used, resulting in the formation of colloidal Pt particles *in situ*. This alkoxide route has several benefits, due to its liquid phase synthesis, including easy mixing of other components into the solution at the atomic level. The synthesis of solutions using SG-derived methodologies is also relatively facile, involving several variables which can be readily manipulated to optimize the films produced. Some of these include the amount of water in the synthesis, the ratio of reactants, the thickness of the film and the film drying temperature. The primary purpose of this paper is to report on the formation and properties of thin, nanoparticulate Pt films using methods typical of SG synthesis. Because metallic nanoparticles are formed, we refer to the process as sol, *vs.* sol-gel, formation, throughout this paper.

Experimental

Synthesis of Pt films.—The synthesis of nanoparticulate Pt films was based on a typical metal salt/ethoxide SG synthesis, involving refluxing under argon a mixture of $H_2PtCl_6 \cdot H_2O$ (Aldrich) and NaC_2H_5O (Aldrich & Alfa Aesar) in molar ratios of 1:1.25 or 1:2.5 in absolute ethanol for 2 h, followed by 18 h of stirring and filtering. Both the supernatant liquid and the precipitate were kept in sealed containers for further testing. Small aliquots of the supernatant were also allowed to evaporate to dryness, and the resulting crystals were retained for testing. Thin films were deposited on substrates using a constant withdrawal rate from the sol, a constant flow rate of sol over the substrate surface, or by deposition of an aliquot of sol with a Pasteur pipette.

Transmission electron microscopy (TEM).—TEM was performed by coating Au or Cu TEM grids (J. B. EM Services, Inc.) with the Pt sol by withdrawal at a slow, controlled rate to ensure the production of a very thin film, through which the electron beam could pass. The coated grids were then dried in air at temperatures ranging between 22 and 400°C for *ca.* 15 min, or for several days when dried at room temperature. The TEM instrument used was a Hitachi H-7000 (Health Sciences Center, University of Calgary).

X-ray photoelectron spectroscopy (XPS).—XPS was used to determine the oxidation state and bonding environment of the Pt in the films. A gold sputtered glass plate was coated with the Pt sol by withdrawal at a rate of 120 cm/min, followed by drying at 190°C for 15 min. Electrochemistry was performed on the lower half of this electrode until the steady-state electrochemical response of Pt was obtained. XPS analysis was then performed on both the upper and lower halves of the sample, using a VG Escalab 200I-XL instrument equipped with a monochromatic Al Kα source.

X-ray diffraction (XRD) analysis.—The films, as well as precipitates collected during Pt synthesis, were examined by XRD. Thick films were formed by deposition of the Pt sol onto a XRD slide, whereas the precipitate was deposited on the slide by first suspending it in acetone, depositing an aliquot onto the slide and allowing the acetone to evaporate. XRD analysis was made of the dried aliquot before and after rinsing for *ca.* 10 s with distilled water and after drying at 200°C for 15 min. Data were obtained using a Siemens D500 Diffractometer with a Kristaloflex 810 X-ray generator (DNX Inc.). Identification was made by comparison with the JADE XRD pattern processing (release 5.0.12) and PCPDFWIN (version 1.20) databases of d-spacings.

Scanning electron microscopy/energy dispersive X-ray analysis (SEM/EDX).—SEM and EDX were used to examine and analyze the larger morphological features and components of the films under study. The films were formed by deposition of the Pt sol on a carbon-covered Al SEM stub, followed by drying at 22°C, or attaching a coated Au sputtered electrode onto the Al stub using silver epoxy. The sputtered electrode was withdrawn from the sol at 60 cm/min and dried at 200°C for 15 min. The bottom half of the films were then cleaned electrochemically until a steady-state cyclic vol-

* Electrochemical Society Student Member.
** Electrochemical Society Active Member.
z E-mail: birss@ucalgary.ca

tammogram (CV) was achieved. SEM/EDX was performed on a Philips FEI XL 30 ESEM in high vacuum mode with a 15 kV acceleration voltage.

Electrochemical measurements.—The electrochemical measurements were performed in a three electrode, two compartment cell using a PARC EG&G 173 potentiostat and 175 programmer. The results were recorded on an HP 7045B X/Y recorder. The counter electrode was a high surface area Pt gauze, while a reversible hydrogen reference electrode (RHE), connected to the main compartment by a Luggin capillary, was employed. All potentials reported here are given *vs.* the RHE. The electrolyte solution was 0.5 M H_2SO_4, deaerated before and during electrochemical measurements by continuously bubbling N_2 through or over the solution. All electrochemical measurements were conducted at room temperature ($22 \pm 2°C$).

The working electrode (WE) substrates used for the electrochemistry of the films were glass slides onto which was sputtered a *ca.* 3 nm layer of Ti followed by a *ca.* 120 nm layer of Au. The Pt film was deposited by dipping the gold sputtered electrodes into the Pt sol and withdrawing it at a controlled rate between 1.2 and 120 cm/min. These electrodes were then dried at 22°C for 24-96 h, or at elevated temperatures (up to 600°C) for 15 min. The apparent area of the coated substrate varied between 0.5 and 1 cm^2. Electrical connection to the WE was made via a Parafilm wrapped alligator clip. Unless otherwise stated, the WE was rinsed with distilled water to remove any water soluble contaminants before being placed in the cell.

Electrochemical experiments were usually initiated at the open circuit potential, *ca.* 0.9 V, and the potential was then swept negatively. Two different regimes were used to achieve a clean, steady-state signal for these Pt films. Either the WE was cycled repeatedly between 0.05 and 1.6 V *vs.* RHE until a steady-state Pt signal was obtained, or the electrode was electrochemically cleaned by cycling between −0.05 and 1.7 V for 3 min at a sweep rate of 1000 mV/s. The more stable films dried at higher temperatures were generally cleaned using the second method.

Quartz crystal microbalance (QCMB) measurements.—QCMB experiments were performed to determine the percentage of the film lost when rinsed with water and after potential cycling, as well as to ascertain the percentage of Pt in the film which is electrochemically active. The AT-cut 5 MHz piezoelectric QCMB crystals (2.5 cm diam, Valpey-Fisher) were sputter coated in the typical ''keyhole'' pattern with a 3 nm undercoating of Ti and a 120 nm layer of Au, giving an area of the overlapping circular areas of *ca.* 0.3 cm^2. Electrical contact was made to the crystal using Au wires attached to the crystal with silver epoxy. The crystal was coated by the application of an aliquot of the Pt sol, deposited on to the crystal surface as the crystal was held at an angle of 60° from horizontal. In all cases, the films were dried either at 22°C for 24 h or at 200°C for 15 min. The crystal was then sandwiched horizontally between two rubber O-rings at the base of the main compartment and electrochemical measurements were carried out as described above. Both the *in situ* and *ex situ* mass measurements were carried out using a Pierce-type oscillator[19] and a Philips PM 66S4C high resolution frequency counter/timer.

Results and Discussion

General observations during Pt sol synthesis.—During the preparation of the Pt sol, the initially orange solution turned black, and was found to consist of a gray/black solid which could be filtered off and a supernatant solution which was yellow/brown in color. The formation of two phases is similar to what occurred during Ir nanoparticle formation,[18] where it was found that the Ir sol remained suspended in a black solution. In the present work, Au electrodes were coated with the solution phase, shown in this work to contain the suspended Pt nanoparticles. When these electrodes were dried at temperatures above *ca*. 200°C, they became black in color. The second phase, the precipitate, was determined to consist of a mixture of NaCl and metallic Pt by XRD[20] and was not studied further in this work.

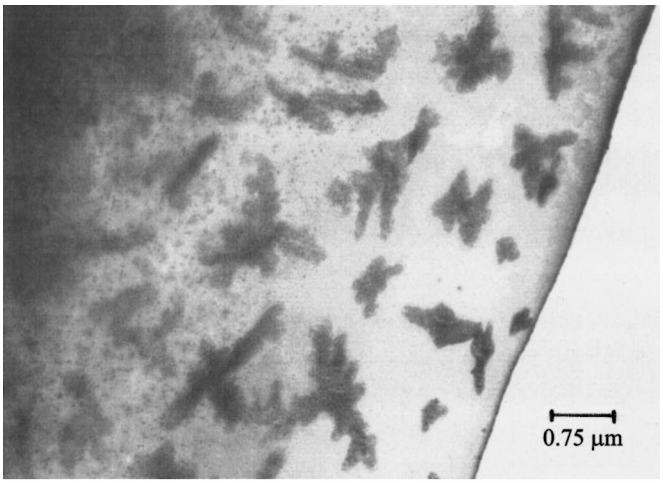

(a)

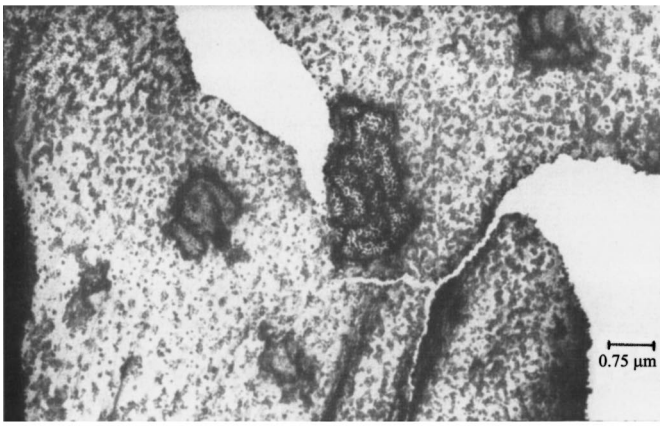

(b)

Figure 1. TEM image of a Pt film formed by withdrawal from a Pt sol and drying at 400°C (a) without subsequent rinsing with water and (b) after rinsing with water.

TEM evidence for presence of Pt nanoparticles.—TEM examinations were carried out of the thin films formed from the sol, as described above. Figure 1a shows a typical low magnification TEM image of the thin edges of the film formed by dip-coating a Au TEM grid from the sol (without subsequent rinsing with water) and dried at 400°C. A crystalline phase, with dimensions of between 0.3 and 1.5 μm, as well as smaller more spherical particles, are seen to be present (at all drying temperatures). However, after rinsing the grid carefully with water, Fig. 1b shows that essentially all of these crystallites have disappeared. These crystallites are either composed of NaCl, an expected product of the synthesis,[20] or of a not fully reduced Pt-containing salt, which is discussed in greater detail in the next section.

Figure 2 shows a TEM of a similar film, but which was dried at 200°C. The larger particles range from 30 to 200 nm in diam., increasing in size as the drying temperature is increased. Careful examination shows that these particles are actually composed of smaller particles which are *ca.* 10-50 nm diam, likely reflecting sintering processes which have occurred as the temperature was increased. Assuming that these particles are composed of Pt metal (see the section on Stability and efficiency of use of the nanoparticulate film), it can be predicted that drying the films at higher temperatures

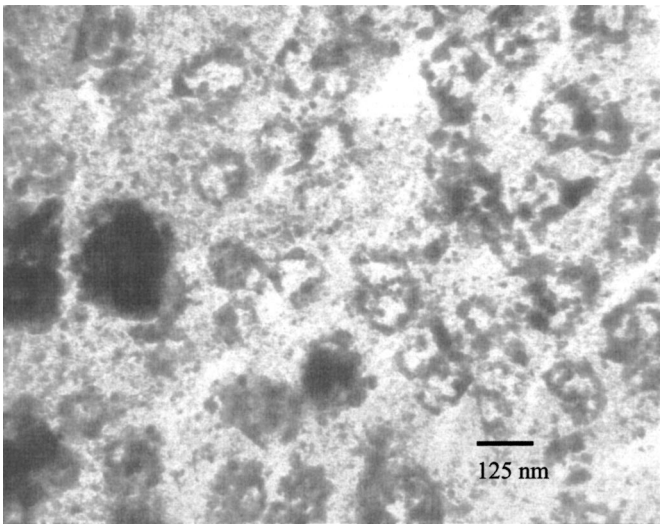

Figure 2. TEM image of a Pt film formed by withdrawal from a Pt sol and drying at 200°C.

will decrease the effective surface area of the film, but should lead to improved stability and electrical contact between particles.

At still higher magnifications, all samples examined by TEM show the presence of a smaller nanoparticulate structure. Figure 3a provides an image of a film dried at room temperature, showing roughly spherical particles of 1-3 nm diam. Figure 3b shows an image of a similar film, but after drying at 400°C, evidence of particles of *ca.* 3-6 nm diam can be seen. The particle size is expected to increase with temperature, similar to what was observed with Ir[18] and other sol-gel derived materials,[21] due to sintering effects. It is shown in the section on electrochemical evidence for Pt thin film formation that this nanoparticulate phase, which remains on the surface after careful rinsing with water, is Pt, based on the electrochemical data obtained. This provides clear evidence that Pt nanoparticles are formed in the solution phase during our synthesis.

Compositional and structural analysis of sol-gel derived Pt thin films .—XPS analysis.—XPS was used to identify the components of the film and their oxidation state. Films studied by XPS were formed by withdrawal of the Au substrate from the Pt sol and were analyzed both before and after electrochemistry. The five important XPS scans of the pre-electrochemistry film, formed by withdrawal from the Pt sol at a rate of 120 cm/min and drying at 190°C for 15 min, with no subsequent rinsing (analogous to the sample examined by TEM in Fig. 2) or electrochemistry, are shown in Fig. 4.

Figure 4a shows that there are at least two different Pt environments in these unrinsed films. The smaller shoulder peaks at 71.1 and 74.5 eV correspond to the metallic Pt 4f shell of spin $\frac{7}{2}$ and $\frac{5}{2}$, respectively.[22,23] The larger peaks, centered at 72.8 and 75.9 eV, indicate the presence of oxidized Pt, likely Pt(II).[22] The larger size of the Pt(II) peaks *vs.* those for Pt(0) indicates that the amount of still-unreduced Pt present is not insignificant, even after drying at close to 200°C. The presence of a Pt species other than Pt metal in these films (and hence in the solution phase formed during sol synthesis) is in agreement with the XRD detection of an unidentified surface compound. The binding environment of the Pt(II) species is not known with certainty, and therefore the compound cannot be identified by XPS.

Peaks in the Cl, C, and O regions of the XPS spectra (Fig. 4b at 199.8 eV, Fig. 4d at 284.0 eV, and Fig. 4e at 532.1 and 535.2 eV, respectively) indicate that the Pt(II) species may be complexed to these elements, *e.g.*, as a Pt chloride ethoxide complex.[20] It can be concluded that it is neither a Pt oxide nor a Pt chloride compound, also ruled out from the XRD results (see the section on XRD analysis). It should be noted that the Au 4f peaks can be detected, indicating that the film is thin (less that the escape depth of the electrons, *i.e.*, <10 nm)[24] or porous. The XPS spectra also exhibit peaks at 198.3 eV (Fig. 4b) and 1072.2 eV (Fig. 4c) ascribed to NaCl,[22] consistent with the XRD and EDX data. Overall, the XPS analysis (Fig. 4) of the freshly formed film (not rinsed, no electrochemistry) indicates the presence of metallic Pt, NaCl, and an unknown Pt(II) compound.

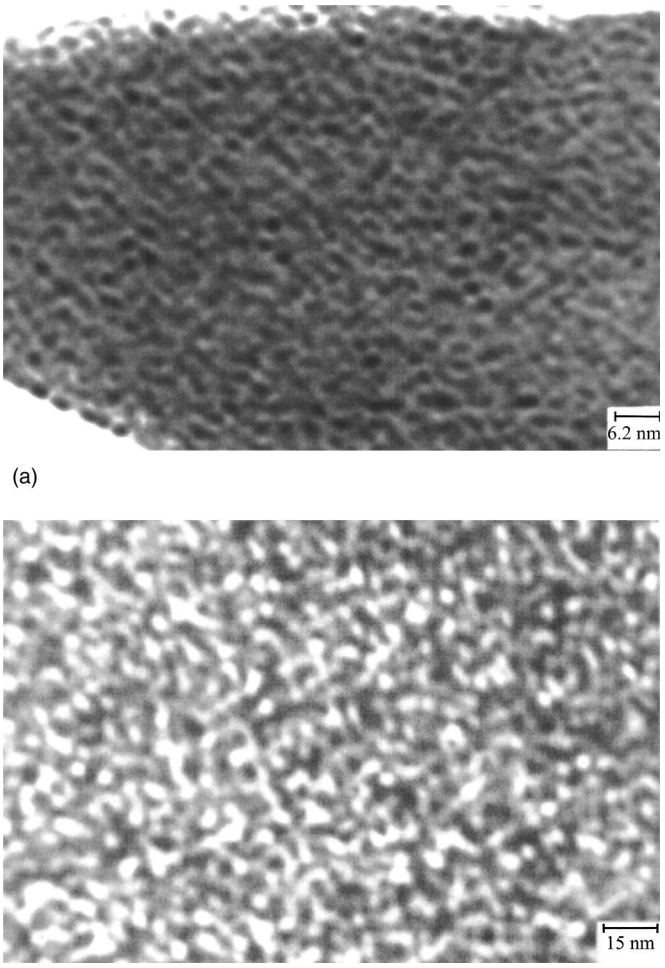

Figure 3. TEM image of Pt films formed by withdrawal from a Pt sol (a) dried at room temperature for 24 h and (b) dried at 400°C for 15 min.

Figure 5 shows the XPS results for the part of the film which had been cycled in 0.5 M H_2SO_4 until a steady-state Pt signal was observed. Unlike the pre-electrochemistry film, (Fig. 4), only the peaks at 70.8 and 74.2 eV, corresponding to the 4f spin $\frac{7}{2}$ and $\frac{5}{2}$ of metallic Pt, respectively, are seen in Fig. 5a. This finding shows that the oxidized Pt(II) compound (Fig. 4a), present in the freshly formed, unrinsed films, dissolves in the acidic solution or is reduced during electrochemical cycling. In the oxygen spectrum (Fig. 5b), only the unidentified peak at 532.1 eV is still seen, while the small peak at 535.2 eV is gone, suggesting that it is linked to the unknown Pt(II) compound. Similarly, there is no longer any evidence for NaCl in the film.

XRD analysis.—XRD was employed to assist in identifying the crystalline components of the thin Pt-containing films, shown in Fig. 1. Figure 6a shows a XRD pattern for a film formed by deposition of an aliquot of the Pt sol on the XRD plate and drying at 22°C for several days, without subsequent rinsing with water. There is no evidence for crystalline Pt from the XRD analysis of this film (at 2θ of 39.75 and 46.2), consistent with the very small size of the Pt

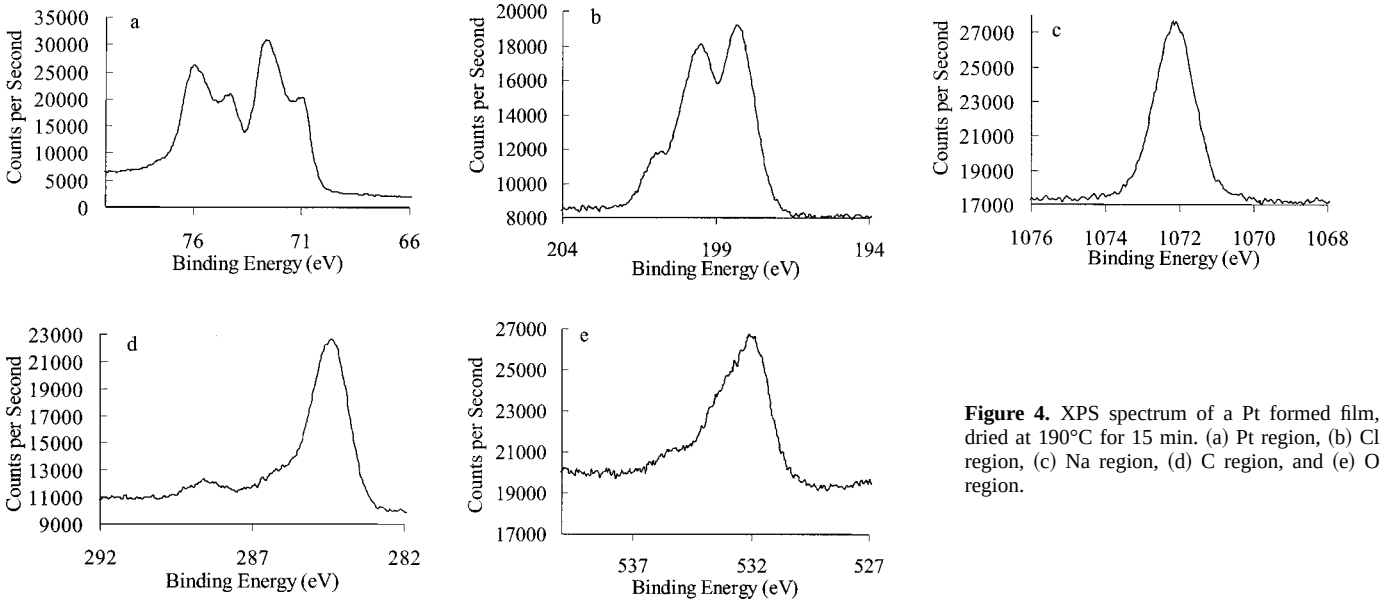

Figure 4. XPS spectrum of a Pt formed film, dried at 190°C for 15 min. (a) Pt region, (b) Cl region, (c) Na region, (d) C region, and (e) O region.

nanoparticles (and hence significant peak breadth,[25] especially after room temperature drying, Fig. 3a). There is at least one well-defined crystalline phase present in this unrinsed film, but all attempts to match it to any known Pt compound or to Na ethoxide in the PCPDFWIN (version 1.20) and JADE (release 5.0.12) databases have failed. (For reference, the XRD spectrum of one of the starting materials, sodium ethoxide, is provided in Fig. 6d.) This film was then rinsed with distilled H_2O for *ca.* 10 s. XRD was again run and the results (Fig. 6b) show that the unidentified crystalline phase [likely the unknown Pt(II) compound seen in the XPS data] dissolves with rinsing (consistent with Fig. 1 and XPS results) and only an unidentified amorphous phase is left behind. A very small peak at $2\theta = 39.88$ may be attributed to metallic Pt. The diameter of these particles can be estimated using the Scherrer equation[25]

$$d = (K\lambda)/(\beta \cos\theta) \quad [1]$$

where d is the diameter of the particles, K is a constant (0.89 for Pt), β is the broadening associated with the peak (measured as the peak width at half-height), λ is the wavelength of the X-ray, and θ is the reflection angle at the maximum peak height. The calculated particle diameter for this film is 4.5 Å, although this is an approximate value due to the low signal to noise ratio of the peak.

A similar Pt film, but dried at 200°C for 15 min, was examined by XRD and the data are shown in Fig 6c. It is seen that at least one of the unknown crystalline products in Fig. 6a has now been thermally decomposed. Significantly, however, the peaks at 2θ of 39.5 and 45.1 correspond to metallic Pt, and have a particle size (Eq. 1) of 6.5 nm, similar to the larger diameter nanoparticles seen in the TEM images of corresponding films. After drying at 200°C, sintering will have caused the nanoparticles to agglomerate, as was seen by TEM and the larger particle diameter calculated *vs.* that for the rinsed films above, now making them detectable by XRD. We thus have further confirmed the presence of nanoparticulate metallic Pt in our sol.

SEM and EDX.—SEM and EDX were used to characterize and identify the larger morphological features in the film. An aliquot of the Pt sol was dried at 22°C for several days on a carbon-coated Al SEM stub, without subsequent rinsing. Figure 7 shows an SEM image of the surface, revealing fracturing of the film at certain sites, typical of either hydrated or sol-gel formed thin films composed of small particles.[21] This fracturing has also caused the loss of regions of the film, which may provide an explanation for some of the mass

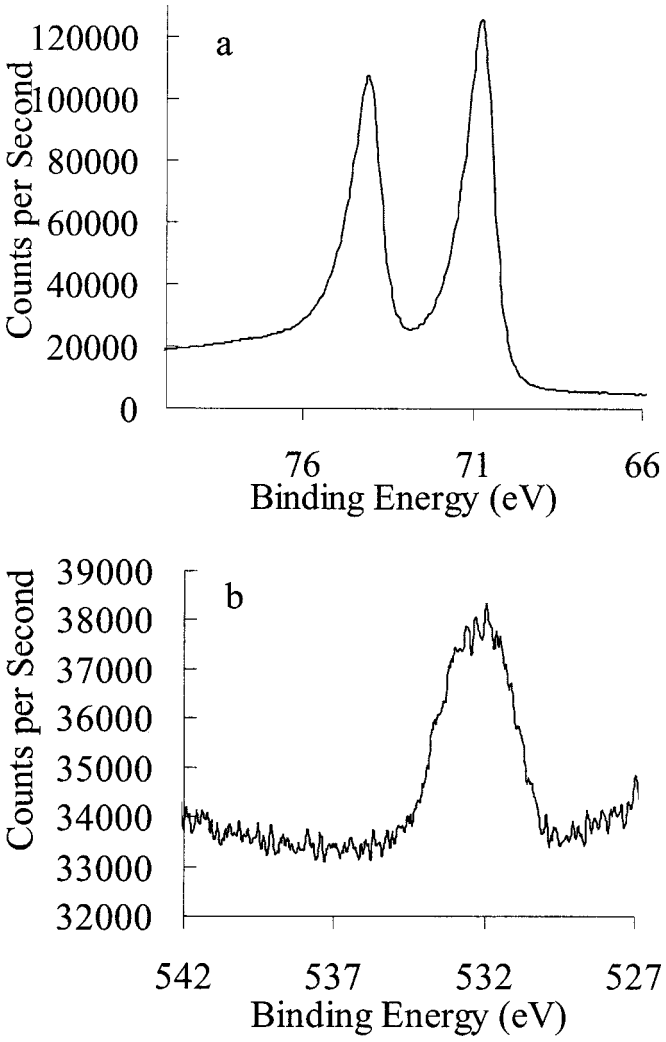

Figure 5. XPS spectrum of a Pt formed film, dried at 190°C for 15 min, and after electrochemistry was run in 0.5 M H_2SO_4 until steady-state CV was obtained. (a) Pt region, (b) O region.

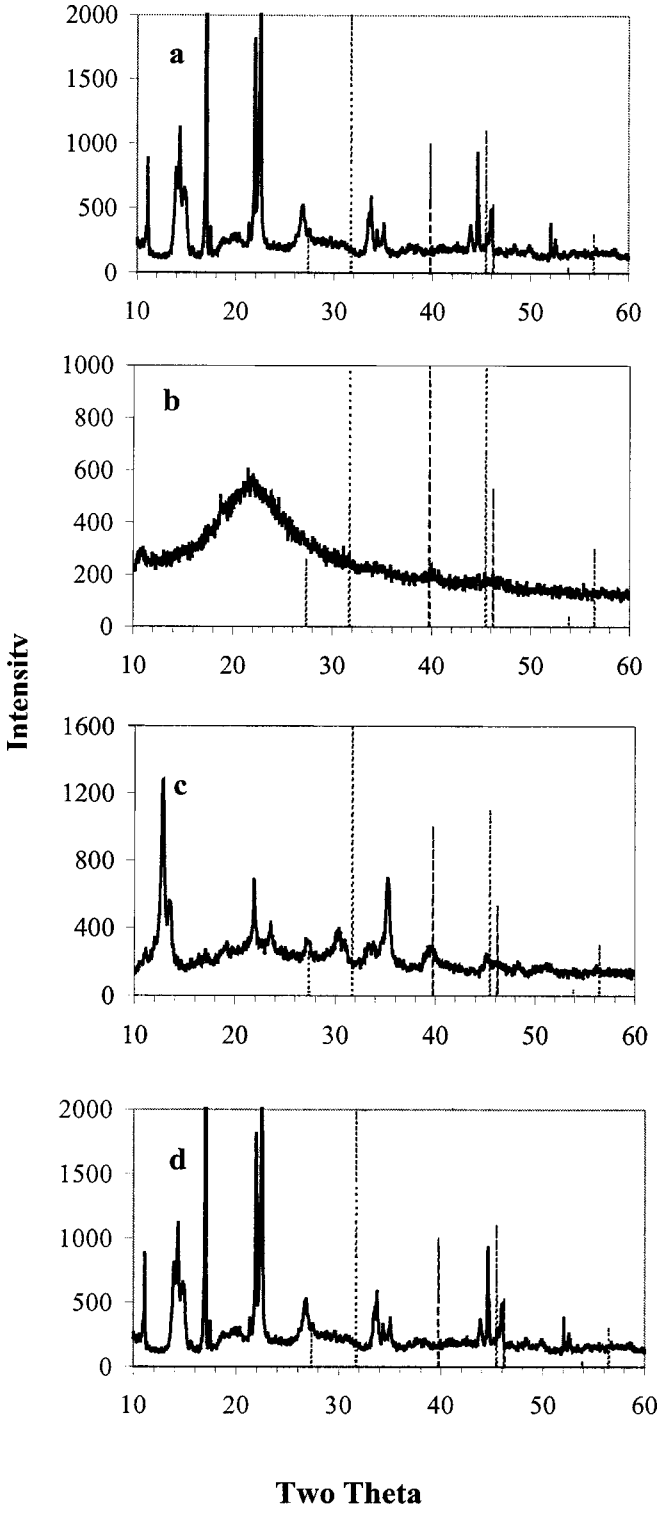

Figure 6. Measured XRD data of experimentally measured Pt sol formed films (——) and the database marker for metallic Platinum (— — —·), and NaCl (· · · ·). (a) Dried at room temperature for 24 h with no subsequent rinsing, (b) dried at room temperature for 24 h, subsequently rinsed with distilled water for *ca*. 10 s, and (c) dried at 200°C for 15 min; (d) sodium ethoxide reference spectrum.

loss (Table I) seen after rinsing or electrochemistry (see the section on Stability and efficiency of use of the nanoparticulate film). EDX analysis performed on regions of the film showed crystalline NaCl, perhaps with some Pt or Pt chloride compound trapped from the

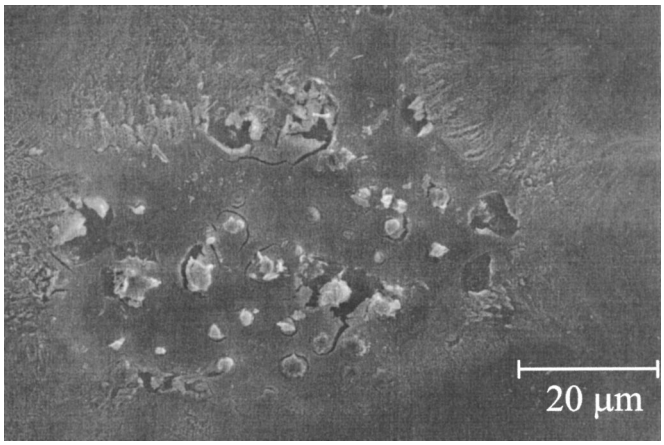

Figure 7. SEM image of a Pt sol formed film, dried at room temperature.

precipitation process. In a few locations, some relatively large particles appear to be composed primarily of Pt, likely due to Pt particle agglomeration. After electrochemical treatment, the NaCl was absent, due to dissolution, and the films were composed primarily of Pt, supporting the XPS findings.

Electrochemical evidence for Pt thin film formation.—Figure 8a shows a typical CV of a polycrystalline Pt-sputtered glass plate in 0.5 M sulfuric acid, revealing the H underpotential deposited (upd) peaks, between 0.05 and 0.4 V, and the Pt oxide growth plateau and reduction peak, centered at 0.8 V. As well, a standard CV for a polycrystalline Au wire electrode is shown. Au was chosen for the substrate to ensure that the H upd peaks which arose from the Pt coating could be used to quantify the electrochemically active Pt area.

In comparison, Fig. 8b shows the initial (0 to 1.6 V) and steady-state CV response of the film material derived from the Pt sol. The film was formed by withdrawing the Au/glass substrate from the sol at a withdrawal rate of 60 cm/min and then drying at 200°C for 15 min. This film was not rinsed before electrochemistry was performed. In the first few cycles, almost full suppression of the Pt CV features is seen. After ~25 cycles between 0.05 and 1.6 V *vs.* RHE, a clean steady-state Pt CV is obtained. There is some evidence for a small net cathodic charge passed in the first few cleaning cycles, perhaps indicating that there is a reducible component present in the initial film [*e.g.*, the Pt(II) compound identified by XPS, Fig. 4]. This excess cathodic charge is most evident in the films dried at room temperature, which are the films that exhibit the greatest amount of blocking during the initial CV cycles. The lower amount of excess cathodic charge in the case of the oven-dried films suggests that the blocking component is removed or decomposed at temperature less than *ca.* 200°C.[20] By comparison with Fig. 8a, the small cathodic peak at ~1.1 V *vs.* RHE is due to the reduction of a small amount of Au oxide, formed at high potentials at the underlying Au substrate, thus demonstrating that the Pt film has some porosity.

To determine the origin of the suppression of the Pt signal in the first few cycles of potential, several Pt sol films were rinsed with distilled water before being tested electrochemically. Rinsing the electrode for approximately 5 s with distilled water, or soaking a film in water for 3 h, produced films which were between 30 and 65% less electrochemically suppressed than films which were not rinsed. Thus, a large portion of this surface contamination is due to the presence of water soluble species (likely NaCl, as seen by SEM, an expected product of the sol formation reaction).[20] This is also consistent with the effect of rinsing of the TEM Au grid in Fig. 1 and the loss of the large, crystalline phase, likely NaCl. Most of the remaining signal suppression (20-50%) may be attributed to ethanol contamination of the Pt surface, as a similar degree of suppression was also exhibited by fresh Pt foil electrodes when dipped in ethanol, dried, and then examined by CV.

Table I. The average measured masses of room temperature dried and oven dried films and the percentage of mass lost during rinsing and electrochemistry of these films.[a] Data shown is the average of at least three samples at each temperature.

Drying temp of film (°C)	Mass per unit area of dry film ($\mu g/cm^2$)	Mass per unit area of film after rinsing ($\mu g/cm^2$)	Percent of original mass lost during rinsing	Mass per unit area of dry film after electrochemistry ($\mu g/cm^2$)	Percent of rinsed mass lost during electrochemistry (% of original mass lost)	Total percent of Mass lost during rinsing and electrochemistry
200°C, 15 min	65 ± 5	58 ± 3	11 ± 2	44 ± 8	23 ± 9 (21 ± 9)	31 ± 7
Room temperature dried, 3 days	123 ± 45	8 ± 3	93.8 ± 0.4	4 ± 2	54 ± 6 (3.4 ± 0.3)	97.1 ± 0.5

[a] Rinsing was completed by spraying the surface with distilled water for several (at least three) seconds. Electrochemistry was carried out until steady-state Pt signal was reached.

The effect of drying temperature on the CV response of these sol-derived Pt films was also examined. Figure 8c shows the CVs obtained after air-drying otherwise identical Pt sol containing films at temperatures between room temperature and 400°C. At lower drying temperatures, less definition is seen in the steady-state H upd peaks, likely attributable to a lower degree of crystallinity in the film and the smaller Pt particle size (Fig. 3). In addition, the room temperature dried films are often less stable, and with extended potential cycling and/or evolution of either oxygen or hydrogen, the CV decreases in size as the Pt particles either dissolve or fall off of the substrate. This is consistent with the larger initial size of the Au reduction peak, indicating a larger exposed fraction of the underlying substrate under these conditions. In contrast, films which have undergone some degree of higher temperature drying are physically much more stable, overall. Other issues related to film stability are examined in more depth in the section on Stability and efficiency of use of the nanoparticulate Pt film.

Figure 9 shows a plot of the steady-state H upd peak charge density as a function of drying temperature for these Pt films, with all other experimental conditions kept constant. It should be noted that the small differences in the H upd peak characteristics (Fig. 8c) as a function of drying temperature may introduce a small error in determining the electroactive surface area, as the normal conversion factor, 0.22 mC/cm^2, is based upon data for bulk Pt.[26] Nevertheless, when this conversion factor is used to calculate the electroactive surface area of these sol-formed thin Pt films, these are between 5 and 20 times higher than for bulk Pt, depending on the sol formation conditions employed.

It can be seen in Fig. 9 that, similar to previous results obtained for SG-derived films of metallic Ir, Ni oxide, and Co oxide,[18,21] the charge density (assumed to be proportional to the electroactive surface area) increases to a maximum at *ca.* 200°C, and then decreases above this temperature. Increasing the drying temperature will initially improve the contact between adjacent Pt particles as well as between the Pt film and the Au substrate as a result of sintering (Fig. 3), thus giving a higher active area and improved film adhesion. As well, at higher drying temperatures (up to 300°C), further conversion of residual still-oxidized Pt complexes (see the next section) to metallic Pt may be occurring, resulting in a film containing a higher proportion of Pt(0) *vs.* when dried at lower temperatures. At temperatures above 200-300°C in Fig. 9, the decreasing charge density is likely due to an overall decrease in surface area, due to the more pronounced sintering effects seen in Fig. 3.

Stability and efficiency of use of the nanoparticulate Pt film.—In order to quantify the loss of water soluble species by rinsing and to further clarify the processes taking place during the CV "cleaning cycles," the film mass was tracked as a function of the experimental conditions employed. In these *ex situ* experiments, the Pt coating was deposited on a Au sputter-coated quartz crystal, and after drying either at room or elevated temperatures, the frequency of the crystals was measured in air and converted to mass per unit area using the Sauerbrey equation (using a crystal constant of 56.6 Hz $cm^2/\mu g$.[19,27]) Once the weight of a freshly deposited, dry, Pt-coated quartz crystal was determined, the crystals were rinsed with distilled water and allowed to dry again in air at room temperature for 24 h, and the mass measurement was repeated. The crystals were then examined electrochemically, and after the film was rinsed and dried, any further mass changes were recorded. As these were *ex situ* measurements, the frequency counter was calibrated on a continuous basis using a standard crystal oscillator to account for any drift in the system.

Table I gives the average mass per unit area of four different samples, all treated identically except for the temperature of drying of the original film. First, it can be seen that the mass of the freshly formed high temperature dried films, without subsequent rinsing or CV cycling, is consistently lower than that of their room temperature dried counterparts. This most likely demonstrates the more complete

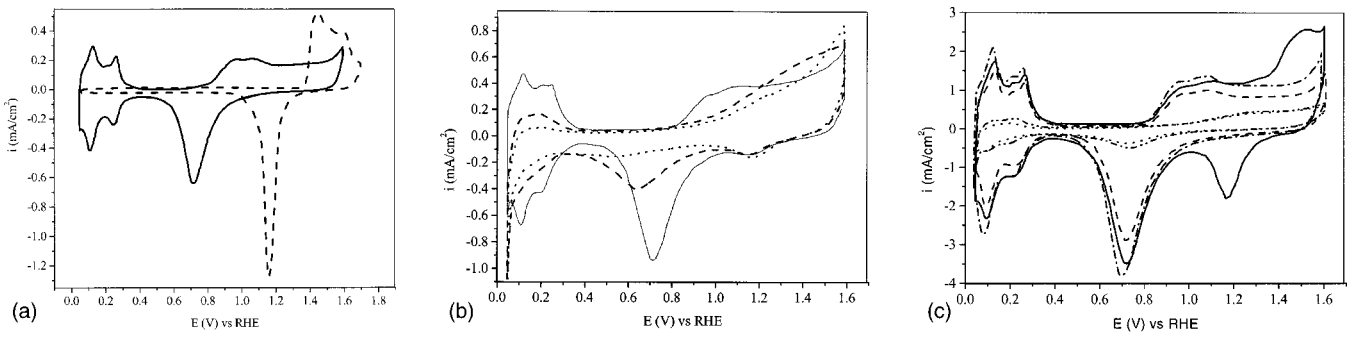

Figure 8. (a) Typical CV of (——) polycrystalline Pt sputtered glass plate, and (— — —) polycrystalline Au wire per apparent area in 0.5 M H_2SO_4. (b) (· · · ·) Initial, (— — —) fifth, and (——) steady-state cycle of a Pt film formed by withdrawal from a Pt sol solution at 60 cm/min, and dried at 200°C for 15 min. (c) CV response of Pt films dried at various temperatures: at (· · · ·) room temperature; (–··–··) 100°C; (–·–·) 175°C; (— — —) 300°C; and (——) 400°C.

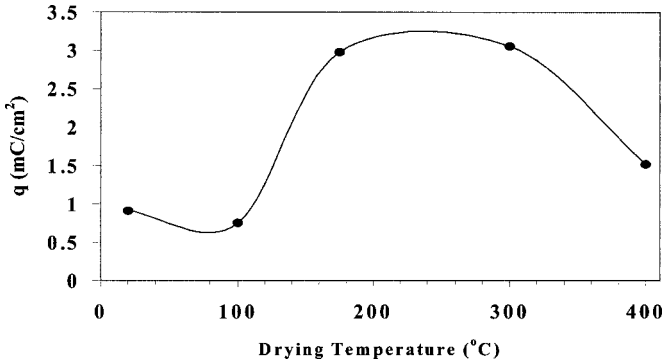

Figure 9. A plot of the steady-state H upd peak charge density per apparent area as a function of drying temperature for the Pt films, with all other experimental conditions kept constant.

removal of solvent and retained organics at these elevated temperatures, consistent with the observations of Fig. 8c and 9. This larger mass loss may also indicate some further conversion of still oxidized Pt complexes to Pt (see the section on Compositional and structural analysis of sol-gel derived Pt thin films).

Upon rinsing with water, Table I shows that all of the films, but particularly the room temperature dried films, lose a sizeable fraction of their mass. This is consistent with the TEM results of Fig. 1, indicating the removal of the crystallite phase, likely NaCl, with water. However, as the TEM results do not show a significantly greater amount of crystallite content after low *vs.* high temperature drying, this suggests that high temperatures also serve to form a more compact and adhesive film.

In situ mass measurements (data not shown) have indicated that, even after rinsing, films lose further mass immediately upon immersion in the acidic solution, and after *ca.* 15-30 min, the film mass reaches a steady state. After potential cycling is initiated, the film again loses mass until a steady-state CV response and mass is obtained. As rinsing serves to remove the NaCl crystallites (Fig. 1), exposure to the acid solution must dissolve some retained Pt salt species and/or to dislodge loosely attached Pt particles from the surface. This would not be surprising, considering the more typical approach of supporting and stabilizing metallic nanoparticles on a porous support material, *e.g.*, carbon.

The film mass data was also employed to provide a very approximate estimate of the film thickness involved in these experiments, by assuming a density of bulk Pt (21.45 g/cm^3). Assuming that these rinsed films are now composed only of Pt, their thickness is 3.6 $\pm$ 1.5 nm and 27 $\pm$ 2 nm, after drying at room temperature and 200°C, respectively (Table II). The films again lose mass during the electrochemical cleaning, and the thickness calculated from the final masses are 1.7 $\pm$ 0.9 nm for a room temperature dried film, and 21 $\pm$ 4 nm for a film dried at 200°C.

Another objective of the QCMB work was to determine what fraction of the Pt nanoparticulate coating is electrochemically active. In these experiments, it was assumed again that the film mass after electrochemistry originates only from metallic Pt, an assumption supported by the XPS data (see the section on XPS analysis). The film mass was used to calculate the total number of moles of Pt in the film, while the electrochemically active Pt (surface Pt) was obtained from the H upd charge, leading to a Pt surface to volume ratio. This ratio was determined to depend on the drying temperature of the films, with the films dried at ~200°C exhibiting a ratio of 0.10 $\pm$ 0.04 *vs.* the room temperature dried films, which showed a surface to volume ratio of 0.13 $\pm$ 0.07.

The theoretical surface to volume ratio calculated based on the average size of the nanoparticles is seen in Fig. 3. For an average nanoparticle diam of 2 nm, the following calculation was carried out. The number of Pt atoms present on the surface of the particle was calculated by dividing the surface area of the particle (1.257×10^{-13} cm^2) by the cross-sectional area of one Pt atom (7.35×10^{-16} cm^2). The number of atoms in the particle volume was calculated by dividing the volume of the particle (4.189×10^{-21} cm^3) by the volume of one Pt atom (1.500×10^{-23} cm^3). At room temperature, the average particle size was 2 nm, yielding an expected ratio of 0.61. However, when dried at 200°C, the particle size increased to an average of 3 nm, with a corresponding anticipated ratio of 0.41. This analysis indicates that the fraction of use is between 20 and 25%, assuming that only the very small particles are electrochemically active.

Conclusions

We have demonstrated that metallic Pt nanoparticles, which remain suspended in solution, can be formed using a sol-gel approach, specifically by the reaction of H_2PtCl_6 with Na ethoxide. The formation of metallic Pt has been confirmed by XRD, SEM/EDX, XPS, and electrochemical studies. The predominant form of this Pt appears to be as nanosized particles, as seen by TEM and confirmed by the large peak width in the XRD spectra and the very large electroactive area *vs.* mass, seen from the cyclic voltammetry/QCMB experiments. We have also shown that the Pt particle size has a strong temperature dependence, with room temperature dried films having an average particle diam of 1-2 nm, while the particle size of the films dried at 400°C is between 3 and 6 nm.

In addition to nanoparticulate Pt, evidence has been found for the presence of some larger Pt nodules (by SEM) in our films, likely indicative of anticipated coalescence of these small particles. As well, another product is formed in the sol-gel reaction, in addition to NaCl. XPS data suggests that it is in the Pt(II) oxidation state, while XRD analyses has been unable to assist in the identification of this material. This product can be partially removed from the surface by rinsing with water and more completely lost by potential cycling in sulfuric acid solutions.

The efficiency of use of our Pt nanoparticles was also determined using sensitive QCMB mass measurements (giving the total Pt weight) together with cyclic voltammetry (yielding the active surface area of the Pt). The active surface to volume ratios have been found to be 0.10 $\pm$ 0.04 for films dried at 200°C and *ca.* 0.13 $\pm$ 0.07 for films dried at room temperature. When compared to the expected ratio of 0.41 and 0.61, respectively, for these films, (based on the Pt nanoparticle sizes seen by TEM), this shows that the overall efficiency of use is between 20 and 25%. These very high

Table II. Average thickness (assuming bulk Pt density) of dip-coated films dried at room temperature and 200°C.[a] Data shown is the average of at least three samples at each temperature.

Drying temperature of film (°C)	Thickness of the original dry film (nm)	Thickness after exposure to water (nm)	Thickness after exposure to water (nm)
Oven dried 200°C, 15 min	65 $\pm$ 5	27 $\pm$ 2	21 $\pm$ 4
Room temperature dried, 3 days	123 $\pm$ 45	3.6 $\pm$ 2	1.7 $\pm$ 0.9

[a] The films were coated by withdrawal from a Pt sol solution at a rate of 60 cm/min, and were rinsed by spraying with distilled water for *ca.* 3 s.

efficiencies of use confirm that the majority of the Pt electrochemical signal must be arising from the Pt nanoparticles.

The temperature at which the films are dried also has a strong effect on the charge density and stability of the film, both of which exhibited an increase between room temperature and 200°C. These increases have been attributed to the conversion of residual oxidized Pt species to metallic Pt and the formation of a more compact and electrically conducting layer at higher temperatures due to particle sintering. At temperatures of 200-300°C, the resulting films are more adherent to the surface, and exhibit a maximum for the charge density, as well as a thickness of close to half that of the room temperature dried films. A decrease in charge density is exhibited at temperatures above this, as the sintering experienced by the Pt particles becomes a dominant factor. It was also seen, using QCMB experiments, that films dried at temperatures of *ca.* 200°C were more structurally stable than those dried at room temperature.

Acknowledgments

The authors thank the Natural Sciences and Engineering Research Council of Canada (NSERC) for the overall support of this research, and for scholarship support of H.A. We would also like to thank the following people for assistance: Marie-Lise Trembley for assistance in the XPS experiments, Rudolf Potucek and Jon McGovern for SEM assistance, and Eric McLeod for his contributions to the electrochemical studies.

The University of Calgary assisted in meeting the publication costs of this article.

References

1. J. M. Hill, R. D. Dortright, and J. A. Dumesic, *Appl. Catal., A*, **168**, 9 (1998).
2. S. Sriramulu, T. D. Jarvi, and E. M. Stuve, *Electrochim. Acta*, **44**, 1127 (1998).
3. L. Liu, V. Rameshkrishnan, R. Liu, and E. S. Smotkin, *Electrochem. Solid-State Lett.*, **1**, 123 (1998).
4. R. A. Periana, D. J. Taube, S. Gamble, H. Taube, and T. S. H. Fuhii, *Science*, **280**, 560 (1998).
5. G. Tamizhmani, J. P. Dodelet, and D. Guay, *J. Electrochem. Soc.*, **143**, 18 (1996).
6. M. Ciureanu and H. Wang, *J. Electrochem. Soc.*, **146**, 4031 (1999).
7. J. B. Goodenough, A. Hamnett, B. J. Kennedy, R. Manoharan, and S. A. Weeks, *Electrochim. Acta*, **35**, 199 (1990).
8. J. Solla-Gullon, V. Montiel, A. Aldaz, and J. Clavilier, *J. Electroanal. Chem.*, **491**, 69 (2000).
9. M. R. Mucalo and R. P. Cooney, *J. Chem. Soc., Faraday Trans.*, **87**, 1221 (1991).
10. S. N. Pron'kin, G. A. Tsirlina, O. A. Petrii, and S. Y. Vassiliev, *Electrochim. Acta*, **46**, 2343 (2001).
11. J. Shan and P. G. Pickup, *Electrochim. Acta*, **46**, 119 (2000).
12. P. G. Allen, S. D. Conradson, M. S. Wilson, S. Gottesfeld, I. D. Raistrick, J. Valerio, and M. Lovato, *Electrochim. Acta*, **39**, 2415 (1994).
13. M. S. Wilson, F. Garzon, H. , K. E. Sickafus, and S. Gottesfeld, *J. Electrochem. Soc.*, **140**, 2872 (1993).
14. M. S. Wilson, J. Valerio, and S. Gottesfeld, *Electrochim. Acta*, **40**, 355 (1995).
15. X. Ren, M. S. Wilson, and S. Gottesfeld, *J. Electrochem. Soc.*, **143**, L12 (1996).
16. S. Y. Cha and W. M. Lee, *J. Electrochem. Soc.*, **146**, 4055 (1999).
17. A. A. Mikhaylova, O. A. Khazova, and V. S. Bagotzky, *J. Electroanal. Chem.*, **480**, 225 (2000).
18. V. I. Birss, H. Andreas, I. Serebrennikova, and H. Elzanowski, *Electrochem. Solid-State Lett.*, **2**, 326 (1999).
19. D. A. Buttry, in *Applications to the Quartz Crystal Microbalance to Electrochemistry*, A. Bard, Editor, Marcel Dekker, Inc., New York (1991).
20. H. Andreas and V. I. Birss, In preparation.
21. I. Serebrennikova and V. I. Birss, *J. Electrochem. Soc.*, **144**, 566 (1997).
22. J. F. Moulder, W. F. Stickle, P. E. Sobol, and K. D. Bomben, *Handbook of X-Ray Photoelectron Spectroscopy*, p. 40, Perkin-Elmer Corp., Eden Prairie, MN (1992).
23. M. Peuckert and H. P. Bonze, *Surf. Sci.*, **145**, 239 (1984).
24. T. A. E. Carlson, *X-Ray Photoelectron Spectroscopy*, p. 214, Dowden, Hutchinson and Ross, Inc., Stroudsburg, PA (1978).
25. B. C. Cullity, *Elements of X-Ray Diffraction*, p. 102, Addison-Wesley Publishing Co. Inc., Don Mills, Ontario (1978).
26. R. Woods, in *Electroanalytical Chemistry*, A. J. Bard, Editor, Marcel Dekker, New York (1976).
27. G. Sauerbrey, *Z. Phys.*, **155**, 206 (1955).